Molecular Materials

DOI: 10.1002/anie.201108919

Antagonism between Extreme Negative Linear Compression and Spin Crossover in $[Fe(dpp)_2(NCS)_2]\cdot py$**

Helena J. Shepherd, Tatiana Palamarciuc, Patrick Rosa, Philippe Guionneau, Gábor Molnár,* Jean-François Létard, and Azzedine Bousseksou*

In memory of Andrés E. Goeta

Although most materials contract under pressure, occasionally a reduction in volume of a material can be achieved by expanding the material in one direction. So-called negative linear compression (NLC)[1] has been previously characterized only in rather simple inorganic[2,3] or organic compounds.[4] NLC is a highly unusual thermodynamic property of a material; to date, only one molecular NLC material has been reported.[4] NLC is the result of specific bonding motifs that may also be responsible for the conceptually related property of negative thermal expansion (NTE).[3,5] As previously noted,[3] NLC has potential applications in composite materials as well as in the development of pressure sensors with very high sensitivity, where the range of applications is vast (such as piezoelectrics). We used high-pressure single-crystal X-ray diffraction and Raman spectroscopy to study a functional molecular material that shows bistability in the form of spin crossover (SCO) between high-spin (HS) and low-spin (LS) states. Intriguingly, a single geometrical mechanism is responsible not only for the strongest NLC behavior yet observed in a molecular material, combined with NTE and extreme positive linear compressibility, but also for the high cooperativity of the SCO in $[Fe(dpp)_2(NCS)_2]\cdot py$ (Scheme 1; dpp = dipyrido[3,2-*a*:2′3′-*c*]phenazine and py = pyridine). The scissor-like motion of individual molecules is propagated through the lattice via the physical intercalation of ligands and is also responsible for suppressing the expected HS→LS SCO under pressure.

Central to the understanding of both NLC and SCO is rationalizing how structural changes affect properties. Cooperative SCO, where the material shows hysteretic thermal spin transitions, is important for many applications[6] and is structural in origin,[7] although the exact link between cooperativity and specific solid state interactions, especially in molecular materials, has often been difficult to rationalize.[8,9] Changes in molecular shape between HS and LS forms and the ability of the crystal lattice to accommodate these changes (elastic properties of the lattice) determine not only the degree of cooperativity, but may also influence whether or not SCO occurs at all.[8] In the field of NLC, extensive efforts have been made towards the rationalization of specific structural and geometric mechanisms that produce this unexpected property, as well as how they can be improved. For example, so-called "lattice-fence" or "wine-rack" motifs[5,10] have been identified to describe the way in which some frameworks form a connected series of hinges that promote this highly anisotropic structural distortion.

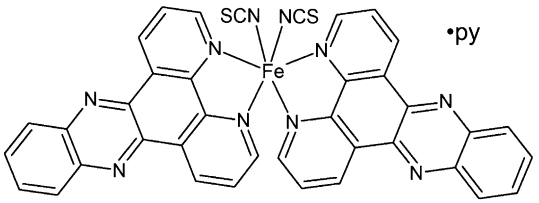

Scheme 1. Structural formula of $[Fe(dpp)_2(NCS)_2]\cdot py$ (**1**; dpp = dipyrido[3,2-*a*:2′3′-*c*]phenazine and py = pyridine).

$[Fe(dpp)_2(NCS)_2]\cdot py$ shows purely thermal SCO with a hysteresis of 40 K ($T_c\downarrow \approx 123$ K, $T_c\uparrow \approx 163$ K),[11] as shown in Figure 1 a. The very abrupt spin transition is accompanied by an isostructural crystallographic phase transition.[12] From HS to LS there is very little decrease in the volume of the unit cell (0.1 %) resulting from the thermal spin transition, in stark contrast to the usual values of between 2 and 10 %;[13] this has been attributed to the anisotropy of the structural rearrangement that accompanies the spin transition.[12] Characteristic cyano stretching (ν-CN) modes of the thiocyanate ligand were used to identify the spin state (HS $\approx 2061\ cm^{-1}$ and LS $\approx 2105\ cm^{-1}$) from pressure-dependent Raman spectra of the material measured at room temperature, as shown in Figure 1. The difference in Raman shift of these characteristic modes between the HS and LS state is the result of the weaker σ bonding and stronger π backbonding on the strength of the CN bond in the HS, as opposed to the LS, state. Such differences are typical for SCO systems and have been suggested to be one of the most convenient probes monitor the spin state in such materials.[14]

[*] Dr. H. J. Shepherd, Dr. G. Molnár, Dr. A. Bousseksou
Laboratoire de Chimie de Coordination, CNRS UPR-8241
and
Université de Toulouse, UPS, INP, Toulouse (France)
E-mail: gabor.molnar@lcc-toulouse.fr
Dr. H. J. Shepherd, T. Palamarciuc, Dr. P. Rosa, Prof. P. Guionneau, Dr. J.-F. Létard
CNRS, ICMCB, UPR 9048, 33600 Pessac (France)
and
Univ. Bordeaux, ICMCB, UPR 9048, 33600 Pessac (France)
E-mail: guio@icmcb-bordeau.cnrs.fr

[**] Financial support was provided by the ANR Project SCOOP (ANR-08-JCJC-0049-01) We are grateful to A. Filhol for the FORTRAN source code of the DEFORM program. dpp = dipyrido[3,2-*a*:2′3′-*c*]phenazine.

Supporting information for this article is available on the WWW under http://dx.doi.org/10.1002/anie.201108919.

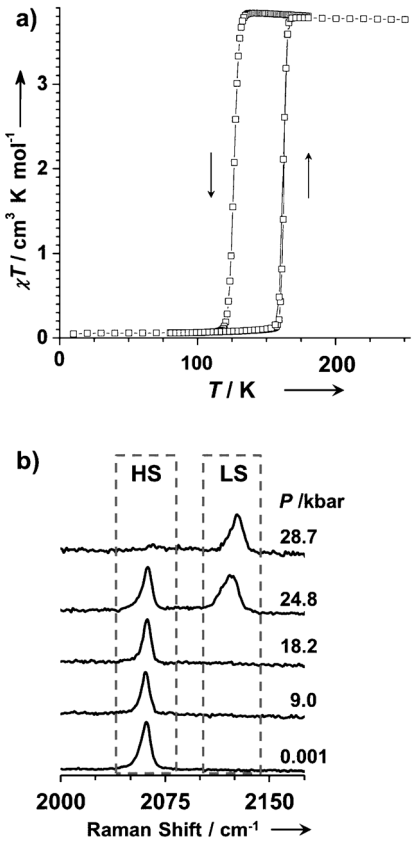

Figure 1. a) Molar magnetic susceptibility in **1** as a function of temperature on cooling and warming, showing spin crossover between HS and LS states. b) Selected normalized Raman spectra of **1** in the CN stretching region between ambient pressure and 28.7 kbar. Additional spectra at intermediate pressures are given in the Supporting Information, Figure S1 c.

Up to and including 18.2 kbar there is no indication of any conversion to the LS state. At 24.8 kbar there is a partial HS→LS conversion, and at 28.7 kbar the crystal has undergone a full SCO to the LS state at room temperature. This is exceptionally high when compared to the related $[Fe(phen)_2(NCS)_2]$ and $[Fe(btz)_2(NCS)_2]$ complexes[15] in which the room-temperature SCO is complete below 10 kbar.[16] Raman spectra show significant structural differences between the HS state and both the low-temperature and the high-pressure LS states (LS_T and LS_P; Supporting Information). On decompression from both 24.8 and 28.7 kbar, the initial HS state returns. High-pressure single-crystal X-ray diffraction was used to rationalize the origin of the very high pressure required to induce the low-spin state.

It is worth starting the discussion of the compressibility of $[Fe(dpp)_2(NCS)_2]\cdot py$ by revisiting the opposing structural effects of cooling and the spin transition on the structure of the HS phase (see the Supporting Information).[12] On cooling the HS state of **1**, the *b* axis and the volume strongly decrease in magnitude. The corresponding thermal expansion coefficients are clearly in excess of the $100\times10^{-6}\,K^{-1}$ threshold suggested for the term "colossal positive thermal expansion":[5] $\alpha_b = +225(2)\times10^{-6}\,K^{-1}$ (the *b* axis being by symmetry an eigenvector of the thermal expansion tensor) and $\alpha_v = 162(1)\times10^{-6}\,K^{-1}$ (see the Supporting Information for derivation and discussion of those values). On the other hand the large increase of the *a* axis shows the presence of NTE behavior. The corresponding eigenvector lies very close to the *a* axis (9°), with an eigenvalue $\alpha_3 = -86\times10^{-6}\,K^{-1}$ that is comparable with the largest reported NTE behavior of between -120 and $-130\times10^{-6}\,K^{-1}$.[5] In stark contrast, the subsequent phase transition accompanying SCO below 150 K causes a significant decrease in *a* (3.5%), and also a striking increase in the *b* axis (13.9%). Upon thermal SCO from HS to LS, the crystal lattice accommodates a drastic change in geometry of the molecule, resulting in a more regular FeN_6 coordination octahedron in the LS phase, as expected.[13] Included in this transition is the large decrease (ca. −15%) of the plane-to-plane angle ψ between the mean planes defined by the atoms of the two dpp ligands towards 90° in the LS_T state.[12]

It is the same geometrical mechanism, a scissor-like opening and closing motion, that accounts for both the highly anisotropic thermal expansion of the HS state (opening) and the structural modifications of the HS→LS phase transition (closing). The orientation of the molecule relative to the unit-cell axes is shown in Figure 2 a, and the resultant scissor-like motion is illustrated in Figure 2 b, which highlights the relationship between the lattice parameters and molecular geometry, as well as how these change during NLC and SCO. At the molecular scale, the opening mechanism observed on cooling the HS state is the same as that on increasing pressure; the geometrical response of the HS molecule to both of these stimuli is the same, albeit with different magnitudes (Supporting Information, Figure S4). This opening mechanism is quantified at the molecular level (in Table 1) by examination of the angle ψ as a function of pressure, derived from single-crystal X-ray structures.[27] The +12% change in ψ demonstrates a strong geometric distortion of the molecule caused by pressure compared to the relatively small distortion caused by cooling of +2%. As pressure increases, ψ increases significantly (Table 1), demonstrating the conflict between the opening induced by pressure ($\psi \approx +12\%$) and closing required for HS→LS_T SCO ($\psi \approx -15\%$). Thus the higher-than-expected pressure required to induce spin crossover can be explained by this mechanism.

The scissor-like opening of the molecule under pressure results in the extreme NLC of the *a* axis shown in Figure 2. This geometrical mechanism is reminiscent of the "wine-rack" motion[5,10] responsible for the NTE and NLC properties observed in other materials. It has been suggested that while there is no thermodynamic necessity for materials with NTE behavior to also show NLC, in practice it is often the case.[5] Indeed, in the present case of $[Fe(dpp)_2(NCS)_2]\cdot py$, both of these highly unusual properties are observed and are attributed to the same mechanism. For the sake of comparison, the very few molecular compounds that show NLC (including those not explicitly reported as having NLC properties) are presented in the Supporting Information. For these compounds we report both the isothermal volume and minimum linear compressibility, defined as the derivative of either cell volume or a cell dimension *l* with respect to

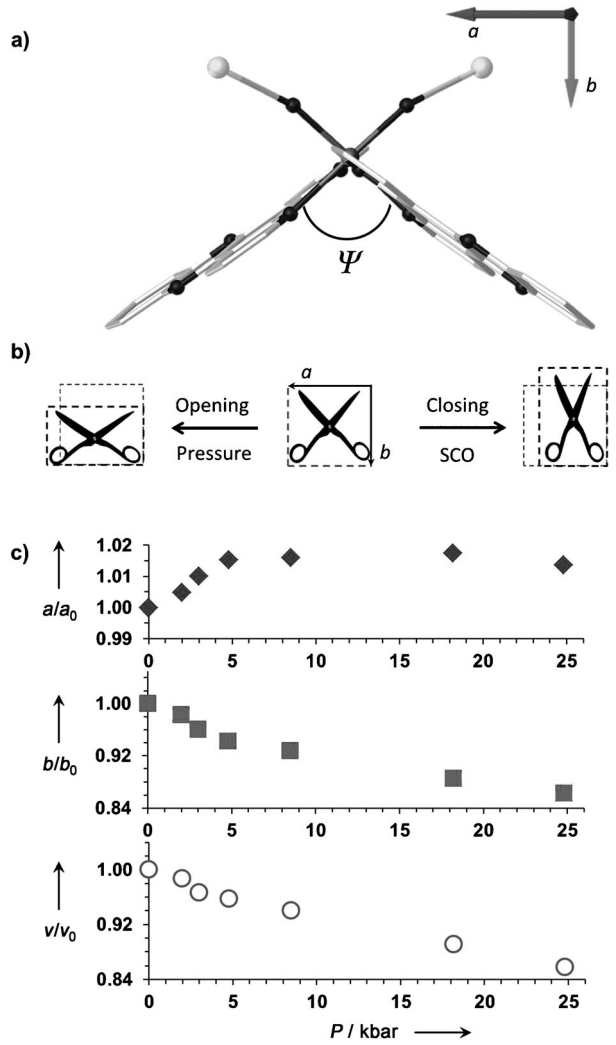

Figure 2. a) View in the *ab* plane of **1** at ambient pressure and temperature showing the relative orientation of the molecule to the unit cell axes and indicating the angle ψ presented in Table 1. Solvent molecules and hydrogen atoms are omitted for clarity. b) Illustration of the "scissor-like" geometric mechanism in the HS state and its effect on the *a* and *b* parameters. Opening is observed upon increasing pressure; closing is associated with a HS→LS phase transition (SCO = spin crossover). c) Relative variation of the a,b axes and unit cell volume of **1** as a function of pressure, showing extreme positive and negative compressibility. Data are derived from high-pressure single-crystal diffraction on two different crystals. Errors on all of the values are contained within the points.

pressure at constant temperature, $K_l = -(\delta l/l\delta p)_T$. Those isothermal compressibilities can also be directly derived from reported elastic stiffness data.[17] Molecular materials with NLC are found to have values of K_l between −2.5 and −20 TPa^{-1}; for a third of these materials, NLC is seen after a pressure-induced phase transition (Supporting Information, Tables S1, S2).

The isothermal compressibility calculated along the *a* axis is $K_a = -30(4)\ TPa^{-1}$. Considering the monoclinic symmetry, the compressibility tensor can be fully determined following the procedure outlined by Filhol et al. (see Supporting Information for details).[18] One strongly negative eigenvalue $K_1 = -41\ TPa^{-1}$ is found with the corresponding eigenvector ca. 26° from the *a* axis.

This tendency becomes less pronounced, though still clearly apparent on further increasing pressure to 18.2 kbar, making the effect significant over a larger range of pressure than previously observed for molecular materials. Another remarkable point is the extreme positive compressibility along *b* up to 4.8 kbar, which we estimated in the same way to be $K_b = +116(13)\ TPa^{-1}$. Despite the substantial NLC, the overall positive volume compressibility of the sample is very high, corresponding to a value of $+94(14)\ TPa^{-1}$. These highly unusual mechanical properties are the result of the opening motion of the molecule that manifests itself in extreme positive and negative responses of the crystal to pressure. This motion at the molecular level also has strong implications for the cooperative nature of the SCO observed in this material.

Physical intercalation of the large, planar dpp ligands with those on adjacent molecules produces a highly cooperative spin transition, rather than π–π stacking interactions as previously suggested.[8,15] The closing motion of one molecule during the spin transition necessitates a complimentary motion in adjacent molecules to accommodate the steric demands of the LS molecule within the lattice. The scissor-like anisotropic distortion of the molecule coupled to physical intercalation of the large dpp ligands is the origin of the highly cooperative interactions observed, as well as for NLC and NTE behavior. The ability of the lattice to accommodate the opposing change in shape of the molecule during the spin transition is what governs whether or not the magnetic HS→LS_T transition can occur. This is essentially an elastic property of the lattice; as the volume of the HS cell contracts by 2% on cooling from 275 to 150 K, the lattice can accommodate the change in shape required for SCO to occur. The same contraction, but with a much greater magnitude (15%) occurs on pressurization up to 18 kbar and the lattice is no longer capable of accommodating the change in geometry. The HS→LS_T transition is thus suppressed but eventually under the application of further pressure a spin transition occurs to LS_P. In all examples of molecular SCO where both the HS and LS structures are known, the HS state is always more distorted than in the LS case.[8,13] We believe that it is because NLC exaggerates this HS distortion in this material that the HS→

Table 1: Structural parameters for **1** as a function of pressure and in the thermal LS state for comparison.[a]

	Thermal LS[b]	HS[c]	Pressure [kbar]						Decompressed from
			2.0	3.0	4.8	8.5	18.2	24.8	24.8 kbar
ψ [°]	92.4(1)	107.22(5)	109.0(1)	111.7(2)	113.0(2)	114.8(2)	118.1(3)	120.1(3)	107.19(7)

[a] For definitions of parameters, see the text and Figure 2a. [b] At 90 K. [c] At ambient temperature and pressure.

LS transition is suppressed, rather than ligand field effects, as demonstrated by the fact that very similar complexes [Fe(phen)$_2$(NCS)$_2$] and [Fe(btz)$_2$(NCS)$_2$][15] undergo SCO at much lower pressures, resulting from the absence of this distortion. As stated above, this scissor-like mechanism resembles the well described[5,10] wine-rack mechanism for NLC, which when extended to consider the supramolecular intercalation of the ligands, connects individual scissors into this type of larger network. The use of supramolecular interactions represents an important tool in the endeavor to design NLC materials with increasingly desirable properties.

In summary, for the first time we have unambiguously shown the microscopic origin of cooperative interactions in a molecular spin-crossover material using a high-pressure structural investigation. Furthermore we have illustrated the antagonistic structural effects of SCO and high pressure on [Fe(dpp)$_2$(NCS)$_2$]·py. These are produced by the same scissor-like geometrical mechanism responsible for both the largest NTE and NCL properties yet reported in a molecular material (along the *a* axis), and the very high positive thermal expansion and linear compressibility (along the *b* axis). The combination of such diverse properties in the same transparent molecular material may be of interest for future optical applications.[1,2,19]

Finally, it is worth highlighting that high-pressure structural investigations of SCO materials are rare,[16,20] but clearly can provide fascinating insights into such molecular materials, in which mechanical properties are often overlooked. These studies provide a formidable tool for uncovering elastic properties in these typically low-symmetry systems, properties which we expect to become increasingly important in the field.

Experimental Section

All of the diffraction data for **1** were collected at room temperature using graphite monochromated Mo K_α radiation ($\lambda = 0.71073$ Å) on an Oxford Diffraction Gemini diffractometer equipped with an EoS detector. Data were processed using CrysAlisPro.[21] Basic models derived from the ambient pressure phase were used as a starting point for refinement of structural parameters against high-pressure data on F^2 using SHELXL-97[22] and Olex2.[23] An absorption correction for the DAC and shadowing from the gasket was applied with Absorb6.1.[24]

Pressure was generated using a diamond anvil cell (DAC) equipped with conical cut diamonds[25] with 800 μm culets. A 250 μm stainless steel gasket with a 350 μm hole was used to form a sample chamber and filled with a silicon oil pressure-transmitting medium. In general, a single crystal of [Fe(bbp)$_2$(NCS)$_2$]·py was loaded inside the chamber along with several small ruby chips. Pressure determination inside the cell was carried out using the ruby fluorescence method.[26] Errors on values of pressure are estimated to be ±0.5 kbar. For diffraction experiments the DAC was mounted on a standard goniometer head. High-pressure diffraction data presented in Figure 2a are from two separate crystals. Further details are given in the Supporting Information.

High-pressure Raman and ruby fluorescence spectra were acquired using a LabramHR (Horiba Jobin–Yvon) microspectrometer. A HeNe laser (632.8 nm) was used as an excitation source; the beam was focused on a spot of approximately 2 μm by a 50× long-working-distance objective. Rayleigh scattering was removed by a holographic notch filter; Raman spectra of the sample were recorded between 200 and 2200 cm^{-1} using a 600 grooves per mm grating with a spectral resolution of about 3 cm^{-1}. The ruby fluorescence spectra were recorded between 687 and 700 nm using the same setup but an 1800 grooves/mm grating, for a spectral resolution of about 1 cm^{-1}.

Magnetic measurements were performed on a polycrystalline sample sealed in a 30 μm-thick polypropylene bag (film courtesy of EXBANOR) on a Quantum Design MPSM-5S SQUID magnetometer. Data measured under 10 kOe were corrected for the sample and the film diamagnetism using tabulated Pascal constants and a previous measurement of the lone film.

Received: December 18, 2011
Revised: February 6, 2012
Published online: March 8, 2012

Keywords: iron · mechanical properties · molecular materials · N ligands · spin crossover

[1] R. H. Baughman, S. Stafström, C. Cui, S. O. Dantas, *Science* **1998**, *279*, 1522 – 1524.
[2] A. L. Goodwin, D. A. Keen, M. G. Tucker, *Proc. Natl. Acad. Sci. USA* **2008**, *105*, 18708 – 18713.
[3] A. B. Cairns, A. L. Thompson, M. G. Tucker, J. Haines, A. L. Goodwin, *J. Am. Chem. Soc.* **2012**, DOI: 10.1021/ja204908m.
[4] A. D. Fortes, E. Suard, K. S. Knight, *Science* **2011**, *331*, 742 – 746.
[5] A. L. Goodwin, M. Calleja, M. J. Conterio, M. T. Dove, J. S. O. Evans, D. A. Keen, L. Peters, M. G. Tucker, *Science* **2008**, *319*, 794 – 797.
[6] A. Bousseksou, G. Molnar, L. Salmon, W. Nicolazzi, *Chem. Soc. Rev.* **2011**, *40*, 3313 – 3335.
[7] H. Spiering, K. Boukheddaden, J. Linares, F. Varret, *Phys. Rev. B* **2004**, *70*, 184106.
[8] M. A. Halcrow, *Chem. Soc. Rev.* **2011**, *40*, 4119 – 4142.
[9] M. Hostettler, K. W. Törnroos, D. Chernyshov, B. Vangdal, H.-B. Bürgi, *Angew. Chem.* **2004**, *116*, 4689 – 4695; *Angew. Chem. Int. Ed.* **2004**, *43*, 4589 – 4594.
[10] J. N. Grima, D. Attard, R. Gatt, *Science* **2011**, *331*, 687 – 688.
[11] Z. J. Zhong, J.-Q. Tao, Z. Yu, C.-Y. Dun, Y.-J. Liu, X.-Z. You, *J. Chem. Soc. Dalton Trans.* **1998**, 327 – 328.
[12] J. Kusz, M. Zubko, A. Fitch, P. Gütlich, *Z. Kristallogr.* **2011**, *226*, 576 – 584.
[13] P. Guionneau, M. Marchivie, G. Bravic, J.-F. Létard, D. Chasseau in *Topics in Current Chemistry: Spin Crossover in Transition Metal Compounds II*, *Vol. 234* (Eds.: P. Gütlich, H. A. Goodwin), Springer, Heidelberg, **2004**, pp. 97 – 128.
[14] J.-P. Tuchagues, A. Bousseksou, G. Molnar, J. J. McGarvey, F. Varret in *Topics in Current Chemistry: Spin Crossover in Transition Metal Compounds III*, *Vol. 235* (Eds.: P. Gütlich, H. A. Goodwin), Springer, Heidelberg, **2004**, pp. 85 – 103.
[15] J. A. Real, A. B. Gaspar, V. Niel, M. C. Muñoz, *Coord. Chem. Rev.* **2003**, *236*, 121 – 141.
[16] T. Granier, B. Gallois, J. Gaultier, J. A. Real, J. Zarembowitch, *Inorg. Chem.* **1993**, *32*, 5305 – 5312.
[17] J. F. Nye in *Physical properties of crystals: their representation by tensors and matrices*, Oxford University Press, Oxford, **1985**, chap. 5, 6 & 8.
[18] A. Meresse, Y. Haget, A. Filhol, N. B. Chanh, *J. Appl. Crystallogr.* **1979**, *12*, 603 – 604; N. B. Chanh, J. Clastre, J. Gaultier, Y. Haget, A. Meresse, J. Lajzerowicz, A. Filhol, M. Thomas, *J. Appl. Crystallogr.* **1988**, *21*, 10 – 14.
[19] J. Sapriel, R. Hierle, J. Zyss, M. Boissier, *Appl. Phys. Lett.* **1989**, *55*, 2594 – 2596.
[20] P. Guionneau, C. Brigouleix, Y. Barrans, A. E. Goeta, J.-F. Létard, J. A. K. Howard, J. Gaultier, D. Chasseau, *C. R. Acad. Sci. Ser. IIc* **2001**, *4*, 161 – 171; P. Guionneau, M. Marchivie, Y.

Garcia, J. A. K. Howard, D. Chasseau, *Phys. Rev. B* **2005**, *72*, 214408; V. Legrand, F. Le Gac, P. Guionneau, J.-F. Létard, *J. Appl. Crystallogr.* **2008**, *41*, 637; H. J. Shepherd, S. Bonnet, P. Guionneau, S. Bedoui, G. Garbarino, W. Nicolazzi, A. Bousseksou, G. Molnár, *Phys. Rev. B* **2011**, *84*, 144107.
[21] CrysAlisPro, Oxford Diffraction Ltd., Version 1.171.33.66.
[22] G. M. Sheldrick, *Acta Crystallogr. Sect. A* **2008**, *64*, 112 – 122.
[23] O. V. Dolomanov, L. J. Bourhis, R. J. Gildea, J. A. K. Howard, H. Puschmann, *J. Appl. Crystallogr.* **2009**, *42*, 339 – 341.
[24] R. J. Angel, *J. Appl. Crystallogr.* **2004**, *37*, 486 – 492.
[25] R. Boehler, K. De Hantsetters, *High Pressure Res.* **2004**, *24*, 391 – 397.
[26] G. J. Piermarini, S. Block, J. D. Barnett, R. A. Foremann, *J. Appl. Phys.* **1975**, *46*, 2774 – 2780.
[27] CCDC 858081 – 858089 contain the supplementary crystallographic data for this paper. These data can be obtained free of charge from The Cambridge Crystallographic Data Centre via www.ccdc.cam.ac.uk/data_request/cif. For further details, see the Supporting Information.

